SIMULATION STUDY ON THE BEAM LOSS MITIGATION IN THE 1ST ARC SECTION OF FRIB DRIVER LINAC*

T. Maruta†, KEK / J-PARC, Tokai, Japan
M. Ikegami, F. Marti, Facility of Rare Isotope Beams, Michigan State University, MI 48824, USA

Abstract

For a high power superconducting (SC) accelerator like FRIB, the extinction of the beam loss inside the cavities is the most important issue for a stable operation. The charge-exchange reaction is unique to heavy ions and potentially generates a loss. Recently we conducted the simulation study to evaluate this loss in the beam transport after 1st linac segment, and then the necessity of one collimation is identified. This paper introduces this study details.

INTRODUCTION

The Facility of Rare Isotope Beams (FRIB) is a high power heavy ion accelerator facility currently being constructed in Michigan State University under cooperative agreement with United States Department of Energy [1]. The driver linac will operate in continuous wave (CW) mode and deliver more than 200 MeV/u all stable heavy ions to the target with beam power of 400 kW.

For a high intensity accelerator, the beam loss mitigation is essentially important. Especially, FRIB intensively employs SC RF cavities after the 0.5 MeV/u Radio Frequency Quadrupole (RFQ), and it is well known that the beam loss inside a SC cavity significantly deteriorates its operable RF voltage. Moreover, the beam loss power density of heavy ions is more severe than proton with same velocity. The energy deposit per unit length is proportional to Q^2/A where Q and A are charge number and mass number, respectively [2]. For example, this density of uranium is 36 times higher than proton. Therefore FRIB must considerably pay attention to potential loss source and distinguish a loss, especially for inside RF cavities for stable operation.

In this paper, we discuss the beam loss originated by charge-exchange reaction in the 1st folding segment (FS1). Since this reaction exchanges a electron with residual gas, the beam ion charge-state, q, varies after the reaction. Then it also varies the magnetic rigidity because it is dependent on the charge-to-mass ratio, q/A. The charge-exchanged ion orbit is distorted and then it could be lost somewhere in downstream. The reaction probability depends on the residual gas pressure. The FS1 is a beam transport connecting 1st and 2nd linac segments (LS1 and LS2). A high power load collimator, namely charge selector, is located in the arc section and pressure level around the selector is estimated to be the worst in the entire driver linac. Therefore significant amount of charge-exchange reaction could occurs around the charge selector. A new collimator position and aperture are optimized by using 3D Particle-In-Cell (PIC) simulation. The simulation studies a charge-exchange reaction of uranium beam. We track the orbits of charge-exchanged ions and loss location in the arc section. Then a new collimator position and aperture size are optimized also by the simulation.

In this paper, the outline of FS1 is explained in the next section. The total power of charge-exchanged ions are estimated from the cross-section and residual gas pressure in 3rd section. The loss location and aperture study by simulation is shown in 4th section. Then we conclude this study in the last section.

FOLDING SEGMENT 1

The FS1 is a 57 m long beam transport connecting parallelly placed 1st to 2nd linac segments (LS1 and LS2) as shown in Fig. 1. The injection beam energy is 16.6 MeV/u for uranium. A charge stripper is placed upstream of the arc section in order to increase effective acceleration gradient at LS2 and later linac section. In the stripper, beam ions are stripped off their electrons by passing though a thin liquid lithium film. The q/A of heavy ions such as uranium increases more than twice. Meanwhile, the beam ions deposit their energy about 0.2 MeV/u on average in the stripper. In the charge stripper, heavy ions with unwanted charge states are also generated. A horizontal movable collimator, namely charge selector, extinguishes these unnecessary ion. This collimator locates after the 1st 45-degree bending magnet in arc section as shown in Fig. 1. The bending radius of each ion differs by their own q/A due to the magnetic rigidity, which is inversely proportional to q/A. Therefore horizontal position at the bending magnet exit depends on each q/A. Moreover, β_x at the selector is minimized to realize a good q/A separation. The arc section is 11 m long, two fold achromatic and isochronous lattice and each of them is comprised from two 45-degree bending, two quadrupole and one sextupole magnets. The beta functions and momentum dispersion along the arc are shown in Fig. 2.

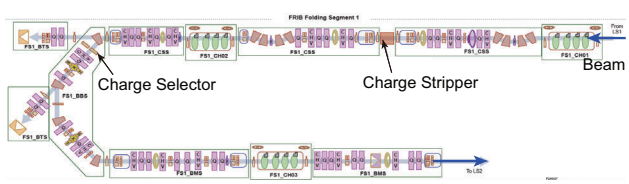

Figure 1: Outline of FS1. The beam is transferred from LS1 (top right) to LS2 (bottom right) passing through 180-degree arc.

* Work supported by the U.S. Department of Energy Office of Science under Cooperative Agreement DE-SC0000661
† tomofumi.maruta@kek.jp

ISBN 978-3-95450-169-4

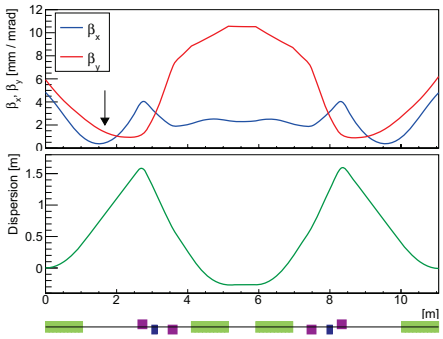

Figure 2: The lattice of the FS1 arc section. The bottom rectangles show the bending (green), quadrupole (purple) and sextupole (deep blue) magnet locations, respectively. Top: Horizontal (blue) and vertical (red) beta functions. The arrow shows the location of charge selector. Bottom: Momentum dispersion function.

CHARGE EXCHANGE REACTION

In this section, we estimate the absolute power of charge-exchange reactions for uranium beam individually. The absolute power is important for a collimator cooling design as well as loss power. There are two kinds of charge-exchange reactions. One reaction is called "electron capture" and abbreviate to EC in this paper. A beam ion picks up one electron from a residual gas molecule, and consequently q decreases by one, $q \rightarrow q-1$, because of negative charge of electron. The other reaction is called "electron loss" because this reaction strips one electron from a beam ion. Thus this reaction increases charge state by one, $q \rightarrow q+1$. We abbreviate this as EL. The fraction of charge-exchanged ions against to initial number of beam ions, R, can be obtained by

$$R = 1 - e^{-\int_0^L \sigma_{tot} n dl}, \qquad (1)$$

where L is beam passing length, σ_{tot} is the total cross-section of the charge-exchange reactions and n is number of molecules of residual gas, respectively. Assuming that the residual gas follows ideal gas law, n is calculated from partial pressure of each gas content. Therefore, absolute power of charge-exchange ions is possible to be calculated from σ_{tot} and pressure along the arc.

Concerning to the cross-sections, we quoted the calculation based on computer simulations [3] due to lack of measurement. In this reference, the correlation of cross-section and energy is fit by a seven free parameters function, and coefficients of the function for both EL (σ_{EL}) and EC (σ_{EC}) are individually listed for nine charge states up to 73+. Here we use the cross-section of 73+ for the estimation. However this charge state is even lower than our design state of 76+ to 80+, we deduce that the cross-sections of our design states are comparable or even lower than 73+. In this high charge state region, the σ_{EC} saturates and the σ_{EL} decreases as charge state being high because electrons are deeply bounded to uranium. The energy dependence of σs for hydrogen and nitrogen molecules are shown in Fig. 3. Obviously, σ_{EL} and σ_{EC} have a different energy dependence. σ_{EL} is very small in low energy and increases like square-root like function and then it almost saturate around 10 MeV/u or higher energy. On the other hand, σ_{EC} is very high in low energy, and exponentially reduces as energy being high. In both reaction, nitrogen cross section is dominant. The cross-sections at 16.4 MeV/u are listed in Table 1, which are calculated from these functions.

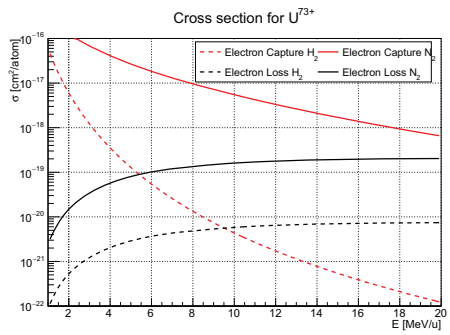

Figure 3: Energy dependence of σ_{EC} (red) and σ_{EL} (black) of U^{73+} ion. Hydrogen (dashed line) and nitrogen (solid line) are selected as a typical residual gas.

Table 1: σ_{EL} and σ_{EC} of U^{73+} at Energy of 16.4 MeV/u

Content	σ_{EL} [cm^2/atom]	σ_{EC} [cm^2/atom]
H_2	7.23×10^{-21}	3.21×10^{-22}
N_2	1.99×10^{-19}	1.23×10^{-18}

The FRIB vacuum group estimated the pressure level of the entire accelerator system. They used a beam line vacuum chamber models by 3D CAD based on the FRIB lattice file. These models provided the geometry to Monte-Carlo simulation code, Molflow+ [4]. They simulated the pressure level of the FS1 arc section and dumped hydrogen and nitrogen partial pressures in 20 mm pitch. The major source of the diffusion in this section is the outgas from the charge selector around 7 m, and it causes the worst pressure of 3×10^{-4} Pa for both gasses as shown in Fig.4. This vacuum pumps placed at 5 m and 10 m are mainly for exhausting these gasses. However the pressure level is comparable in this region, it quickly recovers under 10^{-5} Pa level out of this region. Since this 5 m to 10 m is almost corresponding to the 1st bending magnet to 2nd bending magnet upstream, charge-exchange occurs between these bending magnets.

As already described above, the total charge-exchange reaction can be estimated from the cross section and residual gas pressure level around the charge selector. Since the pressure of each residual gas is dumped in 20 mm step, the R of each step is calculated by Eq. (1) along the arc section. And then integrate the Rs in all steps to get a total fractions. The σ of EC and EL are summed. We only take 1st order reaction. The fraction with hydrogen gas is 5.3×10^{-7} and that with nitrogen is 7.6×10^{-5}, respectively. Then total fraction is 7.7×10^{-5}. When FRIB operates uranium beam

ISBN 978-3-95450-169-4

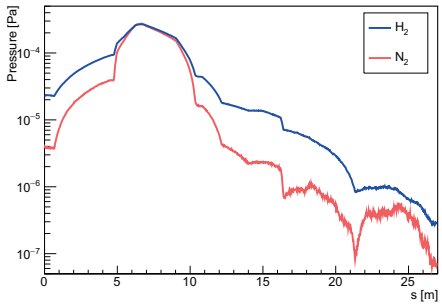

Figure 4: Hydrogen (blue) and Nitrogen (red) pressure in FS1 arc section. The charge selector locates around 7 m where the pressure is the highest.

at design beam power of 400 kW, the beam energy at FS1 is 33 kW. Thus the power of charge-exchanged ions 2.5 W.

SIMULATION

The two step simulation study is conducted to identify the loss location. The 1st step is a simulation of beam ions along the arc section because beam ions are source of charge-exchange reaction. The 3D PIC code, IMPACT [5], is employed for the simulation. The U^{76+} to U^{80+} ions are generated at the 1st bending magnet entrance with design beam profile. Then these ions are simulated step-by-step along the arc section without space charge force. Number of particles is 20 k in total and fraction of each charge states follows Baron's formula [6]. The position, momentum vector and q/A of all ions are dumped at the entrance, exit and inside the magnetic elements between the 1st to 2nd bending magnets. The orbit of charge-exchanged ions inside magnets must be different from the beam due to different q/A.

The 2nd simulation is played with dumped beam information in the 1st step. The q of all ions are modified by $+1$ or -1 to represents EL or EC respectively. The fraction of $+1$ and -1 follows the ratio of σ_{EL} and σ_{EC} and pressure of dumped location. Then the simulations are restarted from all dumped locations and tracked envelopes to the arc end. All simulated horizontal envelopes of charge-exchanged particles are superimposed to one figure to confirm a loss location, and then we noticed that these ions are lost around sextupole and quadrupole magnets in latter half of the arc section as shown in Fig. 5. The envelope of charge-exchanged ions is gradually wide from the 2nd bending magnet, and then it is quickly divergent after the 3rd bending magnet. The loss location is near the peak of momentum dispersion as shown in Fig. 2.

We consider the optimum collimator position from this result. The charge-exchanged ions are well separated from the primary beam in high momentum dispersion area. The loss starts from 3rd quadrupole downstream and location could shift upstream is momentum distribution is wider than design. Consequently, we decided placing a horizontal collimator at 3rd bending downstream. The collimator aperture is determined to be ±20 mm as shown in Fig. 6. In this aperture, no loss occurs in the arc section as well as the collimator has a sufficient tolerance of about 6 mm from

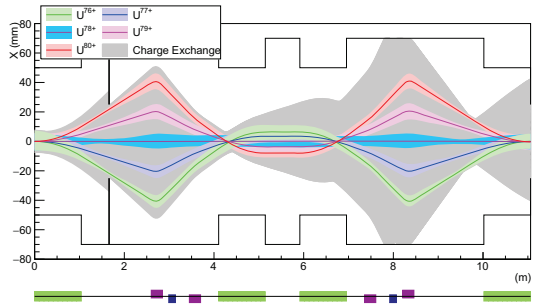

Figure 5: The envelope of charge-exchanged ions (gray) in the arc section, the uranium beam envelopes of five charge states are also superimposed as a reference.

beam tail. The power deposit to this collimator is 1.9 W. We also tracked the orbit of charge-exchanged ions in the LS2 during the aperture optimization, and it is confirmed that no loss occurred inside SC cavities.

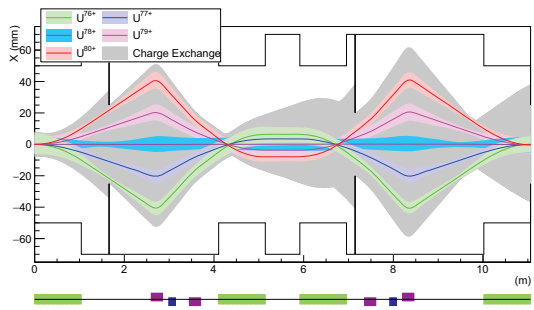

Figure 6: The envelope of charge-exchanged ions (gray) with additional collimator in the arc section.

CONCLUSION

The charge-exchange reaction is the specific loss source for heavy ion accelerator. However the simulation study clarified that this reaction in the FS1 arc section potentially generates a watt-order loss, this loss is successfully mitigated by placing a horizontal collimator in the arc section.

REFERENCES

[1] J. Wei *et al.*, "FRIB accelerator status and challenges", in *Proc. of LINAC'12*, Tel Aviv, August 2012, p. 417.

[2] Y. Yamazaki *et al.*, "Beam physics and technical challenges of FRIB driver linac," in *Proc. of IPAC'16*, Busan, Korea 2016, p. 2013.

[3] V.P. Shevelko, M.-Y. Song, I.Yu. Tolstikhina, H. Tawara, and J.-S. Yoon, "Cross sections for charge-changing collisions of many-electron uranium ions with atomic and molecular targets," *Nucl. Instr. Meth.* B278 pp. 63–69, 2012.

[4] A. Müller and E. Salzborn, "Scaling of cross sections for multiple electron transfer to highly charged ions colliding with atoms and molecules," *Phys. Lett.*, 1977, 62A, 391-394.

[5] J. Qiang, R.D. Ryne, S. Hbib, and V. Decyk, *J. Comput. Phys.* 163 (2000) 434.

[6] E. Baron, M. Bajard, and Ch. Ricaud, *Nucl. Instrum. Methods. Phys. Rev.* **A238**, 177 (1993).

ISBN 978-3-95450-169-4